J Mol Model (2013) 19:3427–3436
DOI 10.1007/s00894-013-1857-1

ORIGINAL PAPER

Incomplete mixing versus clathrate-like structures: A molecular view on hydrophobicity in methanol–water mixtures

Sven P. Benson · Jürgen Pleiss

Received: 21 February 2013 / Accepted: 16 April 2013 / Published online: 18 May 2013

Abstract The underlying molecular mechanisms of macroscopic excess properties were studied by molecular dynamics simulations for different compositions of methanol–water mixtures. Structural data (nearest neighbor relationships, clustering analysis) and dynamic data (hydrogen bond lifetimes, rotational autocorrelation, translational diffusion) were evaluated. Nearest neighbor relationships provide quantitative evidence and a pictorial description of incomplete mixing at the molecular level as a source for mixture anomalies, while a comparative study of water surrounding methyl moieties versus water in the bulk-like environment provides evidence against the hydrophobicity model of clathrate-like hydration. Furthermore, the formation or breakdown of the system-wide hydrogen bonding network at a critical threshold of approximately equimolar mixture is perceived to separate the mixture system into two hydrogen bonding regimes: hydrogen-bonded water clusters embedded in methanol for mixtures with low water content and methanol molecules within a system-wide hydrogen-bonded water network for mixtures with high water content.

Keywords Excess properties · Hydrogen bonding network · Hydrophobicity · Incomplete mixing · Percolation

Introduction

Deviations from ideal mixture behavior (excess effects) in aqueous solutions are a widespread phenomenon that is quantified mostly by macroscopically observable properties such as entropy [1]. However, measuring macroscopic observables does not explain the molecular origin of the anomalies in mixtures, which results from the nature of the intermolecular interactions of the different molecule types. Solution chemical reaction rates, ion transport in solution or membranes, protein folding and enzymatic activity are but a few instances where an in-depth understanding of molecular mechanisms is of paramount importance. Excess effects in aqueous solutions are generally ascribed to hydrophobicity. While hydrophobicity is a useful chemical concept, even after decades of detailed investigation the underlying molecular mechanisms are still controversial [2, 3]. As prevalent and intuitive as "hydrophobicity" may seem, it is important to note that hydrophobicity is not a first-principle parameter, but an abstract concept. The terminology of "hydrophobicity" in itself is misleading, because it implies a lack of attraction between polar water molecules and nonpolar groups, when in fact attractive interactions persist due to induced dipoles [4]. The cause of hydrophobicity is widely attributed to the comparatively strong electrostatic attraction between water molecules via hydrogen bonding [2, 3]. In this connotation, "hydrophobicity" is best described as the "hydrophilicity" of water in preference to molecules with weaker dipoles.

One of the most seminal works on molecular association behavior in aqueous solutions is that of Frank and Evans [5] published in 1945, which introduced the model of "ice-like" clathrate structures of immobilized water molecules surrounding nonpolar moieties. Kauzmann [6] later correlated the hydrophobic interaction with protein folding and stability and introduced it as a driving force for structural assembly and phase separation in solution. While these ideas undoubtedly had profound influence on the perception of how water interacts with nonpolar solutes on a molecular level, the scientific evidence is inconclusive and thus the molecular mechanisms of hydrophobicity are still a topic of

Electronic supplementary material The online version of this article (doi:10.1007/s00894-013-1857-1) contains supplementary material, which is available to authorized users.

S. P. Benson · J. Pleiss (✉)
Institute of Technical Biochemistry, University of Stuttgart,
Allmandring 31,
70569 Stuttgart, Germany
e-mail: Juergen.Pleiss@itb.uni-stuttgart.de

high controversy. Evidence for immobilized water molecules has been found, e.g., in early neutron diffraction experiments [7–9] and Monte Carlo simulations [10]. However, more recent molecular dynamics simulations [11], ab initio calculations [12, 13] and diffraction experiments [14, 15] have contested these findings.

Incomplete mixing has been proposed as an alternative concept to explain the molecular source of excess properties in aqueous mixtures [1, 14, 16]. In contrast to the localized immobilization of water surrounding nonpolar solutes of the clathrate model, incomplete mixing explains excess entropy by a system-wide molecular segregation.

Hydrophobicity is widely perceived to be a multifaceted problem that manifests itself differently dependent on the interface between the hydrophobic compound and the aqueous environment, such as fully miscible liquids, small micelles, proteins in solution, or fully separated phases [2, 3]. In aqueous solutions, hydrogen bonds are perturbed when small nonpolar solutes are introduced to the mixture, which leads to a structural rearrangement of water molecules (entropic effect). In contrast, large hydrophobic interfaces are perceived to reduce the number of possible hydrogen bonds in the system (enthalpic effect). This differentiation however seems arbitrary, considering that structural rearrangement of water molecules would also take place in the presence of large hydrophobic interfaces, while likewise the number of possible hydrogen bonds in solution would eventually decrease as the concentration of small nonpolar solutes increases.

To study hydrophobicity and the molecular mechanisms of excess effects with molecular dynamics simulations, we chose water–methanol mixtures as simple model systems.

Methods

Simulation details

MD simulations were performed at 298.15 K and 1 bar under periodic boundary conditions in an NPT ensemble. The Berendsen coupling scheme [17] was used, with coupling constants of 0.4 ps for temperature and 1.2 ps for pressure coupling. The leap-frog algorithm [18] was used for all simulations with a time step of 2 fs. C-H and O-H bond lengths were constrained with the LINCS algorithm [19]. Long-range electrostatics was treated by the particle-mesh Ewald algorithm (PME) [20, 21]. Lennard-Jones interactions were capped at 1.4 nm. The transferable all atom optimized potential for liquid simulation (OPLS) force field [22] was used for methanol; water was parameterized by the TIP4P model [10]. During an equilibration phase of 20 ns, energy, density, and radial distribution functions were monitored, followed by a production phase of 10 ns for analysis. The GROMACS 4.0.7 software was used for simulations and analysis [23, 24].

Molecular self-diffusion coefficient

The molecular self-diffusion coefficient $\boldsymbol{D}_A$ is a transport property that describes the translational mobility of particles A and can be regarded as a meaningful quantity to link molecular mobility to the macroscopic deviation from ideal mixture behavior witnessed in excess properties [25]. It is calculated from the mean-square displacement and the Einstein relation by averaging over all particles [26].

$$\lim_{t\to\infty}\left\langle (\mathbf{r}_i(t)-\mathbf{r}_i(0))^2\right\rangle_A = 6D_A t \tag{1}$$

Nearest neighbor relationships

To characterize changes in local structure for the different compositions of a binary methanol–water mixture, the deviation of the nearest neighbor relationships in the simulated systems from their expected values in an ideal mixture was calculated. Nearest neighbor relationships were defined by a radial cutoff criterion of 0.35 nm (Online resource Fig. S1). $\boldsymbol{N}_{ix}^{\text{total}}$ denotes the total number of molecules (methanol and water) that are neighbors to molecule centers of type i (either methanol or water). $\boldsymbol{N}_{ii}^{\text{ideal}}$ denotes the number of water-water or methanol-methanol neighbor relationships as expected in an ideal mixture. In a fully randomized molecule distribution, $\boldsymbol{N}_{ii}^{\text{ideal}}$ may be calculated from $\boldsymbol{N}_{ix}^{\text{total}}$ and the molar fraction χ_i by

$$N_{ii}^{ideal} = p_{ii}^{ideal}\cdot N_{ix}^{total} = \chi_i \cdot N_{ix}^{total}, \tag{2}$$

where $\boldsymbol{p}_{ii}^{ideal}$ denotes the probability of finding a neighbor of molecule type i to a molecule center of type i for an ideally randomized molecule distribution, assuming that the difference in molecule size of both molecule types in the system is negligible (ideal mixture criterion). In an ideal mixture, $\boldsymbol{p}_{ii}^{ideal}$ should be equal to the molar fraction χ_i of molecule type i. In an ideal binary mixture, the number of nearest neighbors between two molecules of different types $\boldsymbol{N}_{ij}^{ideal}$ (the number of neighbors of molecule type j to centers of molecule type i) is calculated by:

$$N_{ij}^{ideal} = N_{ix}^{total} - N_{ii}^{ideal} = (1-\chi_i)\cdot N_{ix}^{total} (i \neq j). \tag{3}$$

The deviation between simulated (real) and ideal mixtures can thus be quantified by the ratios $\boldsymbol{M}_{ii}$ and $\boldsymbol{M}_{ij}$:

$$M_{ii} = \frac{N_{ii}^{real}}{N_{ii}^{ideal}} = \frac{N_{ii}^{real}}{\chi_i \cdot N_{ix}^{total}} \text{ and } M_{ij} = \frac{N_{ij}^{real}}{N_{ij}^{ideal}} = \frac{N_{ij}^{real}}{(1-\chi_i)\cdot N_{ix}^{total}}, \tag{4}$$

with N_{ii}^{real}, N_{ij}^{real}, and N_{ix}^{total} being derived from the simulation. M_{ii} is therefore a quantity to describe the association bias of molecules *i* within a binary mixture and the resulting structural arrangement of the two molecule types. Likewise, M_{ij} characterizes the interaction between the different molecule types. In M_{ij}, the first index *i* signifies the central molecule type and *j* the neighboring molecule type ($M_{ij} \neq M_{ji}$). For ideal binary mixtures we expect $M_{ii}=1$ and $M_{ij}=1$, while for incomplete mixing we expect $M_{ii}>1$ if molecules of type *i* favor the proximity to molecules of the same type and $M_{ij}>1$, if molecules of type *i* favor the proximity to molecules of the other type *j*.

Hydrogen bond lifetime

Upon separating water molecules into a clathrate-like water and a bulk water group, it is necessary to take heed of water molecules quickly leaving the first water shell around the methyl moieties due to fast translational diffusion. To circumvent this difficulty, the evaluation of correlation times provides a simple and descriptive property to compare the duration of the existence of a signal. Therefore, the hydrogen bond (HB) correlation function $c_h(t)$ [27] was analyzed,

$$c_h(t) = \frac{\langle h(0)h(t)\rangle}{\langle h\rangle}, \tag{5}$$

where h denotes the existence function and $\langle h\rangle$ the total population of HBs. The existence function equals unity if a HB exists and is zero otherwise, under the condition that $h(0)=1$. This HB lifetime description has been called the "intermittent hydrogen bond correlation function" [28], alluding to the fact that by construction it is time-independent of bond-breaking events. From the correlation of the existence function it is possible to define the reactive flux correlation function $K(t)$ [27].

$$K(t) = \frac{dc_h(t)}{dt} = kc_h(t) - k'n(t) \tag{6}$$

The term $k'\,n(t)$ describes bond-breaking and the term $k\,c_h(t)$ bond-forming. From here on it is possible to define the HB lifetime τ_h as the inverse of the forward rate constant *k*.

$$\tau_h = \frac{1}{k} \tag{7}$$

Rotational autocorrelation

The rotational autocorrelation time can be calculated by integration or fitting of the rotational autocorrelation function $C_h(t)$.

$$C_h(t) = \langle P_n[u(0)\cdot u(t)]\rangle \tag{8}$$

P_n is the rank n Legendre polynomial and $u(t)$ a vector associated with the geometry of the molecule to be analysed. Specifically the normal vector to the water molecule plain $u(t)=r_{OH1}$ x r_{OH2} was used [29]. Applying the rank 2 Legendre polynomial makes calculated data comparable to experimental NMR data [30, 31]. Instead of integration, the trapezoidal rule was used to acquire the Riemann sum between intervals of discrete time steps of 2 fs.

Differentiation of clathrate-like and bulk water molecules

To determine whether there is a difference in the dynamics of water molecules surrounding nonpolar methyl moieties (clathrate-like water) and free water molecules (bulk water) within methanol–water mixtures, the two groups were analyzed separately. Clathrate-like water molecules were assigned by applying a distance cutoff criterion between the carbon atom of methanol and the oxygen atom of water, where 0.45 nm corresponds to the first minimum of the radial distribution function g(r) [Cmet-Owat] (Online resource Fig. S1). The full simulation trajectories were segmented into equally long parts of 500 ps and were analyzed after redefining clathrate-like and bulk water for every segment. Since the long tail of autocorrelation functions significantly influences results, a combined scheme of explicit integration until 5 ps and fitting after 5 ps was applied, which has previously been benchmarked for similar systems [29]. For mixtures below $\chi_{wat}<0.6$, water molecules could no longer be separated into clathrate-like water and bulk water groups when applying the cutoff criterion of 0.45 nm, because all water molecules were assigned to the clathrate-like water group from thereon. Therefore, the cutoff criterion was reduced to 0.35 nm, which corresponds to the first peak maximum of g(r) [Cmet-Owat]. Reducing the cutoff criterion to 0.35 nm resulted in a shift of the exponential increase of HB lifetimes τ_{ww} from $\chi_{wat}\sim0.5$ to $\chi_{wat}\sim0.2$ (Online resource Fig. S2), which suggests that the water molecules in the outer half (0.35 nm–0.45 nm) of the first coordination sphere statistically mask the effect of exponentially rising HB lifetimes from $0.5>\chi_{wat}>0.2$. The large standard deviations at low water content are a consequence of the small number of bulk water molecules.

Results

Multiple molecular dynamics simulations were performed on condensed phase systems containing pure water, pure methanol and nine intermittent methanol–water mixtures (χ_{wat}=0.0, 0.1, 0.2, …, 1.0). The molecular systems were equilibrated thoroughly (20 ns), while monitoring potential energy, density, and radial distribution functions. A system size of 1000 molecules with periodic boundary conditions

proved sufficient for analysis, since simulations of larger systems led to comparable results (Online resource Fig. S3). To explore the molecular basis for deviations from ideal mixture behavior, all simulations were analyzed for structural properties such as density (Online resource Fig. S4), radial distribution functions (Online resource Fig. S1/S3), nearest neighbor relationships, clustering analysis and dynamic properties such as molecular self-diffusion, rotational autocorrelation and hydrogen bond (HB) lifetimes. Molecules surrounding the nonpolar methyl moiety (clathrate-like water) and "free" water molecules (bulk water) in the methanol–water mixtures were separated into two groups and analyzed individually when appropriate, in order to implicitly assess increased order of clathrate-like water as a possible source for the lower than expected entropy in the mixture.

Diffusion coefficient

Molecular self-diffusion coefficients for methanol and water molecules were analyzed to capture excess behavior on a molecular level and to compare simulation results to experimental data (Fig. 1).

For low molar fractions of water, the diffusion coefficient of water molecules was found to be high ($\boldsymbol{D}_{\chi wat=0.1}$=2.02 10^{-5} cm^2/s) and decreased with increasing water content to a minimum at $\chi_{wat}\approx0.5$ ($\boldsymbol{D}_{\chi wat=0.5}$=1.81 10^{-5} cm^2/s). For $\chi_{wat}>0.5$, the coefficient increased again until the maximum value ($\boldsymbol{D}_{\chi wat=1.0}$=3.59 10^{-5} cm^2/s) for pure water was reached (experimental: $\boldsymbol{D}_{\chi wat=1.0}$=2.16 10^{-5} cm^2/s [32]). Similarly, the diffusion coefficient of methanol was found to be high for low molar fractions of methanol ($\boldsymbol{D}_{\chi met=0.1}$=2.14 10^{-5} cm^2/s). It decreased with increasing methanol content until a minimum at $\chi_{met}\approx0.4$ ($\boldsymbol{D}_{\chi met=0.4}$=1.81 10^{-5} cm^2/s) and increased again until the maximum of $\boldsymbol{D}_{\chi met=1.0}$=2.96 10^{-5} cm^2/s for pure methanol (experimental: $\boldsymbol{D}_{\chi met=1.0}$=2.5 10^{-5} cm^2/s [32]). Thus, the minima of the diffusion coefficients for water and for methanol were both found in the vicinity of χ_{met}=0.4–0.6 (χ_{wat}=0.4–0.6) of the mixture, while the highest diffusion coefficients were found for the pure substances.

Diffusion coefficients are also a meaningful quantity to probe for variations in translational mobility between clathrate-like water and bulk water, which is a possible source for the lower than expected entropy observed for methanol–water mixtures. However, water molecules in both groups displayed no discernible difference in diffusion coefficients and were in close agreement with the diffusion coefficient presented for all molecules (Fig. 1). This suggests that there is no significant difference in translational mobility between clathrate-like water and bulk water. Compared to experimental values [33], the simulated diffusion coefficients were consistently overestimated, but the relative trend was adequately represented. These findings are in agreement with previously published data [29, 34].

Rotational autocorrelation

To compare the dynamics of clathrate-like water and bulk water, the rotational autocorrelation time τ_w for a vector orthogonal to the water molecule plane was separately analyzed for clathrate-like water and bulk water. Water molecules in the clathrate-like water and bulk water groups displayed similar rotational correlation times τ_w for all mixture compositions, ranging from τ_w (χmet=0.1)=1.83 ps to τ_w (χmet=0.9)=3.94 ps (Fig. 2), which is in agreement with

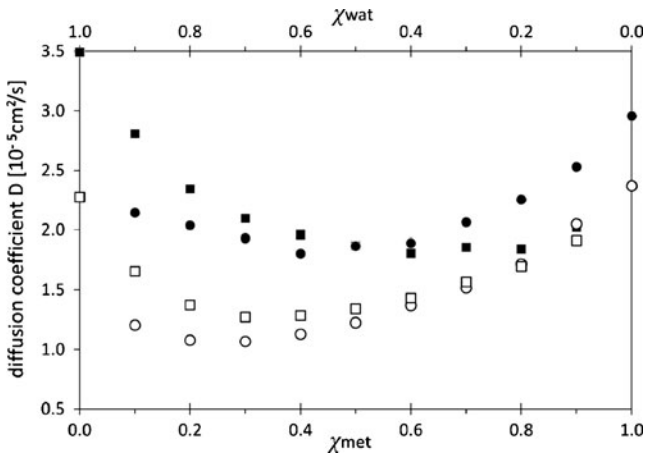

Fig. 1 Molecular self-diffusion coefficients **D** in methanol–water mixtures for simulated water (TIP4P: *black square*), experimental water [32] (*white square*), simulated methanol (OPLS/AA: *black circle*) and experimental methanol [32] (*white circle*). Simulation data was obtained from mean square displacement and the Einstein relation. Standard deviation and detailed statistics of the calculations are provided in Online resource (Fig. S5)

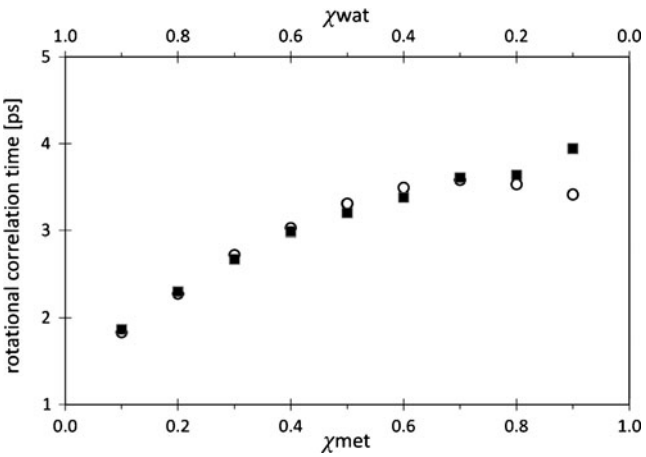

Fig. 2 Rotational correlation time τ_w of the normal vector to the water molecule plain in methanol–water mixtures calculated via the integral of the rotational autocorrelation function (rank 2 Legendre polynomial) of the clathrate-like water group (*white circle*) and the bulk water group (*black square*), after applying a spherical differentiation cutoff criterion for clathrate-like water of 0.35 nm around the methyl group. Standard deviations averaged over multiple trajectory intervals range from 0.01–0.1 ps

experimental values of τ_w (χmet=0.0)~2.0 ps [30, 31] and simulation data of TIP4P water model literature of τ_w (χmet=0.0)=0.8–1.7 ps [29].

A linear increase for $0.1<\chi_{wat}<0.5$ and a convergence to maximal values for $0.5<\chi_{wat}<0.9$ was observed.

Hydrogen bond lifetimes

The hydrogen bond (HB) lifetime τ can be regarded as a characteristic quantity for the dynamics of hydrogen-bonded clusters (Fig. 3a).

For pure water, HBs between water molecules had a short lifetime (τ_{ww}(χwat=1.0)=1.47 ps). Upon decreasing water content in the methanol–water mixture, the lifetime of water-water HBs increased linearly up to an equimolar ratio (τ_{ww}(χwat=0.5)=4.4 ps). When decreasing the water content further ($\chi_{wat}<0.5$), τ_{ww} increased almost exponentially until a maximum at $\chi_{wat}=0.1$ was reached (τ_{ww}(χwat=0.1)= 10.39 ps). In contrast, the lifetime of HBs between methanol molecules τ_{mm} changed only slightly for the different mixtures. HB lifetimes were short for low methanol content (τ_{mm}(χmet=0.1)=1.17 ps) and slightly increased to τ_{mm}(χmet=0.6)=2.6 ps just above equimolar composition. For higher molar fractions of methanol, the lifetime remained at almost constant levels between τ_{mm}=2.6–3.06 ps. The lifetimes of HBs between methanol and water τ_{mw} were found at levels between τ_{ww} and τ_{mm}, with a linear increase from τ_{mw}(χmet=0.1)=1.8 ps to τ_{mw}(χmet=0.1)=5.72 ps.

When comparing water molecules in clathrate-like water and bulk water groups, we found lifetimes τ_{ww} of bulk water to be significantly higher than τ_{ww} of clathrate-like water for $\chi_{wat}<0.5$ when applying a differentiation cutoff criterion of 0.45 nm (Online resource Fig. S6) and $\chi_{wat}<0.2$ when applying a cutoff criterion of 0.35 nm (Fig. 3b).

Nearest neighbor relationships

To find evidence for incomplete mixing at the molecular level, nearest neighbor relationship analysis between molecules within the methanol–water mixtures was performed by examining the ratios $\boldsymbol{M}_{ii}=\boldsymbol{N}_{ii}^{real}/\boldsymbol{N}_{ii}^{ideal}$ and $\boldsymbol{M}_{ij}=\boldsymbol{N}_{ij}^{real}/\boldsymbol{N}_{ij}^{ideal}$ between the number of neighbors in the simulated ($\boldsymbol{N}_{ii}^{real}$) mixtures and the calculated values for ideal mixtures ($\boldsymbol{N}_{ii}^{ideal}$) (Fig. 4).

The neighbor relationships $\boldsymbol{M}_{ww}$ (central water molecule to water neighbors), $\boldsymbol{M}_{wm}$ (central water molecule to methanol neighbors), $\boldsymbol{M}_{mm}$ (central methanol molecule to methanol neighbors) and $\boldsymbol{M}_{mw}$ (central methanol molecule to water neighbors) were analyzed for all methanol–water mixtures. Starting from $\boldsymbol{M}_{ww}$=1.00 at χ_{wat}=1.0 (pure water), $\boldsymbol{M}_{ww}$ increased upon decreasing the water content, until $\boldsymbol{M}_{ww}$= 1.21 was reached at χ_{wat}=0.3 and then remained constant. Conversely, $\boldsymbol{M}_{wm}$ (water–methanol neighbors) was consistently lower than ideal levels at the same mixture compositions as $\boldsymbol{M}_{ww}$, with a minimum of $\boldsymbol{M}_{wm}$=0.72 at χ_{wat}=0.9. Thus, in all methanol–water mixtures the water molecules preferred other water molecules as neighbors rather than methanol molecules (positive bias). Unlike the water-water nearest neighbor relation, $\boldsymbol{M}_{mm}$ (methanol-methanol neighbors) decreased upon decreasing the methanol content, starting from $\boldsymbol{M}_{mm}$=1.00 at χ_{met}=1.0 (pure methanol) until $\boldsymbol{M}_{mm}$= 0.67 at χ_{met}=0.1. $\boldsymbol{M}_{mw}$ (methanol–water neighbors) was consistently higher than ideal levels at the same mixture compositions as $\boldsymbol{M}_{mm}$, with a maximum of $\boldsymbol{M}_{mw}$=1.51 at χ_{met}=0.9.

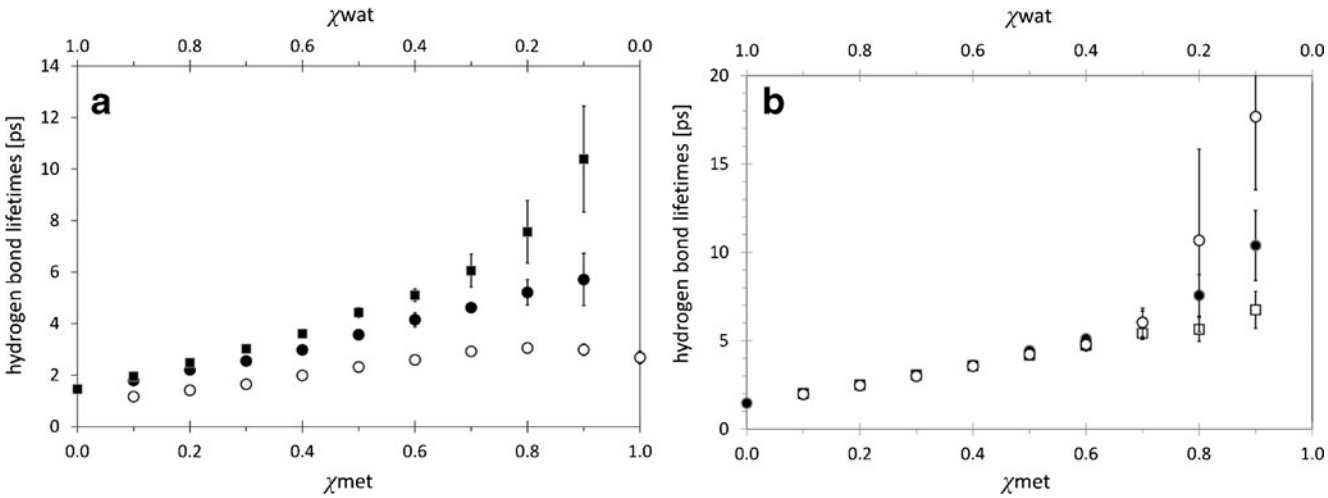

Fig. 3 Hydrogen bond lifetime τ in methanol–water mixtures as the inverse of the forward lifetime of the autocorrelation function (ACF) for (**a**) interactions water-water τ_{ww} (*black square*), methanol–water τ_{mw} (*black square*), methanol-methanol τ_{mm} (*white circle*) and (**b**) interactions water-water τ_{ww} of the clathrate-like water group (*white square*), the bulk water group (*white circle*) and all water molecules (*black square*), after applying a spherical differentiation cutoff criterion for clathrate-like water of 0.35 nm surrounding the methyl group. Error bars display standard deviations averaged over multiple trajectory intervals

Thus, methanol molecules display the tendency to disfavor other methanol molecules as neighbors (negative bias), but prefer water molecules. We therefore witness demixing of methanol and water molecules within the molecular system, with water being the preferred neighbor to both water and methanol molecules.

Cluster formation

An analysis of largest clusters was conducted to assess hydrogen bond percolation in the methanol–water mixture system, by applying a single-linkage algorithm with a spherical distance cut-off criterion of 0.35 nm (hydrogen bonding cutoff criterion) between oxygen atoms. Since the size of largest clusters vary during simulation, the largest cluster N_{max} and the smallest cluster N_{min} found throughout the entire simulation for each molar fraction was determined, as well as the average largest cluster size $N_{aver.}$ The methanol cluster sizes (Fig. 5b) decreased from N_{aver}=25 (χ_{met}=1.0) to N_{aver}=2 (χ_{met}=0.1).

The overall largest clusters were significantly larger for the entire range of mixture compositions, spanning from N_{max}=89 (χ_{met}=1.0) to N_{max}=8 (χ_{met}=0.1), whereas the overall smallest cluster spanned from N_{min}=12 (χ_{met}=1.0) to N_{min}=1 (χ_{met}=0.1). In general, an exponential decrease of largest cluster size for decreasing methanol content was observed. In contrast, the size of water largest clusters (Fig. 5a) hyperbolically decreased for high water content from N_{aver}=996 at χ_{wat}=1.0 to N_{aver}=421 at χ_{wat}=0.6, until an inflection point was reached close to equimolar mixture (χ_{wat}=0.5) with N_{aver}=107. From thereon, an exponential decay was observed for χ_{wat}<0.5 until the minimum at N_{aver}=4 (χ_{wat}=0.1). The deviations of the overall largest and smallest clusters found throughout the analysis did not vary as dramatically for water as they did for methanol, except in the vicinity of the inflection point, where N_{max}=542 (χ_{wat}=0.6) and N_{min}=98 (χ_{wat}=0.6).

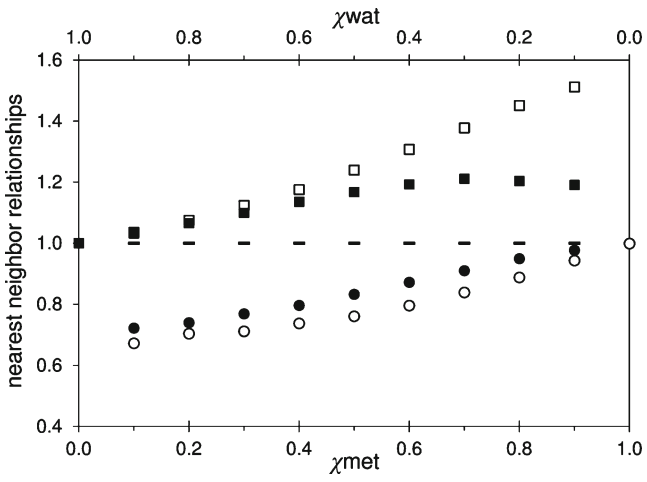

Fig. 4 Nearest neighbor relationships between water and methanol molecules within a cutoff distance representative of hydrogen bonding (0.35 nm) are presented for methanol–water mixtures by the relation $\mathbf{M}_{ii}=\mathbf{N}_{ii}^{real}/\mathbf{N}_{ii}^{ideal}$ of neighbors $\mathbf{N}_{ii}^{real}$ found for simulated mixture systems to neighbors $\mathbf{N}_{ii}^{ideal}$ expected for ideal mixtures of the same composition. Bias in the mixture systems due to molecular interactions is perceived relative to ideal mixture expectations (dashed line)—interactions: water-water $\mathbf{M}_{ww}$: *black square*/methanol–water $\mathbf{M}_{mw}$: *white square*/water–methanol $\mathbf{M}_{wm}$: *black circle*/methanol-methanol $\mathbf{M}_{mm}$: *white circle*. Standard deviations averaged over multiple trajectory intervals range from 0.15 to 3.45

Discussion

Incomplete mixing versus clathrate-like structures

The Frank and Evans model postulates increased structural order of water molecules surrounding nonpolar moieties in aqueous solutions, which, if it held true, could clarify the molecular basis of hydrophobicity in general and the lower than expected entropy of methanol–water mixtures in particular. Clathrate-like hydration is a highly controversial topic. While some investigations of aqueous solutions confirm the existence of clathrate-like hydration [35–38], others have found no evidence for structural rearrangement of water molecules surrounding nonpolar solutes in aqueous solutions [39–45]. Indeed, excess entropy in methanol–water mixtures was recently quantified solely based on radial distribution functions reflecting molecular-scale segregation within methanol–water mixtures, “without the need to invoke icebergs” [1]. It should be possible to determine if clathrate-like water structures contribute to excess entropy by comparing dynamic properties of clathrate-like water and bulk water molecules. Indeed, Dzugutov et al. proposed a formalism that directly correlates diffusion and entropy [25, 46]. Particularly, reorientational correlation of water molecules has been widely used to investigate the existence of immobilized hydrate water, but immobilization could also affect translational diffusion. Therefore, differences in the dynamics of clathrate-like and bulk water are a necessary condition of the Frank and Evans model. Mere structural observations such as the existence of water clathrates around methanol molecules are insufficient to support the model. Pratt’s statement that “clathrate is in the eye of the beholder” [47] frames this consideration nicely, by suggesting that while conceiving clathrate-like structures may not be necessary for a quantitative description of thermodynamic properties in aqueous solutions, if you look for them then you are likely to find them. Despite this premise, we did not find clathrate-like structures when comparing translational, rotational dynamics and HB lifetimes of molecules in the clathrate-like water group with molecules in the bulk water group. Our results are therefore in agreement with findings that refute clathrate-like structures as a source of excess entropy in methanol–water mixtures [39–45].

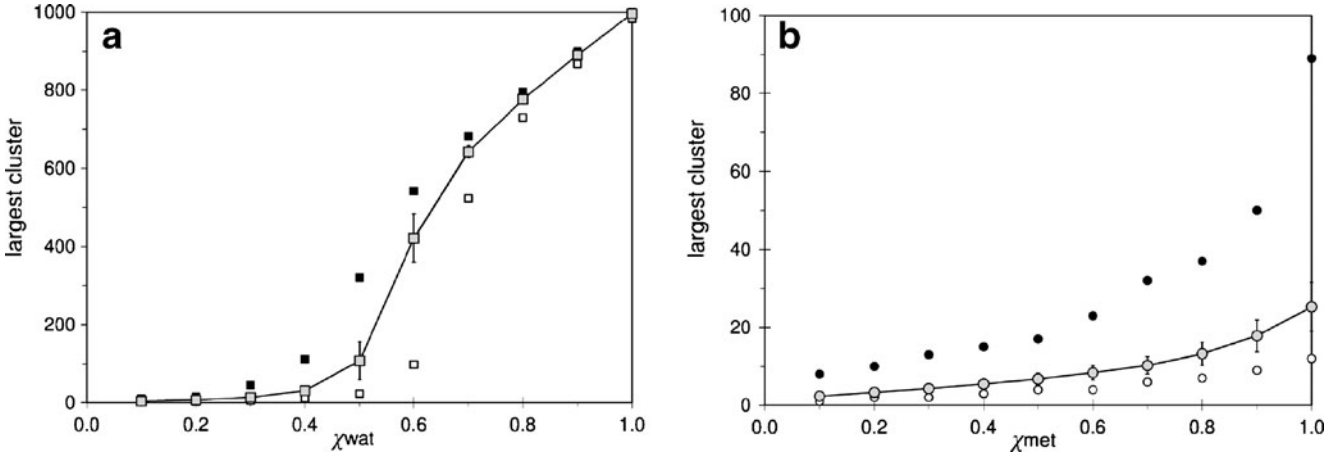

Fig. 5 Clustering analysis of molecules in methanol–water mixtures using a spherical cutoff criterion of 0.35 nm for (**a**) largest clusters of water molecules (biggest overall cluster: *black square*/largest cluster on average: *black square*/smallest overall cluster: *white square*) and (**b**) for largest clusters of methanol (biggest overall cluster: *black circle*/largest cluster on average: *black circle*/smallest overall cluster: *white circle*). Error bars display standard deviations averaged over multiple trajectory intervals

In spite of the sizable evidence against clathrate-like structures and the fact that quantitative theories in support of clathrate-like hydration are scarce [48], the Franks and Evans model has remained popular in the general perception of hydrophobicity and is still the focus of widespread investigation. Human intuition plays an important role in science as a catalyst for the development of new ideas and in this regard a pictorial model is certainly more inspiring than less intuitive models like an abstract comprehension of the superimposition of proximal radial information that contradicts clathrate-hydration [1]. The conception of an equally simple and pictorial alternative model that accounts for the molecular origin of hydrophobicity without incorporating clathrate-hydration would be desirable. Thereby it is certainly not sufficient to merely disprove existing clathrate models, which appears particularly challenging due to the abundance of inconclusive and contradictory findings.

The concept of incomplete mixing [1, 14, 16] lays its focus on molecular-scale segregation throughout the mixture rather than localized structural arrangements. It is widely recognized and also confirmed by our results that molecular segregation in aqueous solutions is driven by hydrogen bonding preference. For methanol–water mixtures, the observed positive bias of the water-water association and the negative bias of the methanol-methanol association, as well as the preference of methanol to associate with water as a neighbor were demonstrated by nearest neighbor relationships. It indicates that the distinctive preference of water as a hydrogen bonding partner leads to a system-wide change in structural order within methanol–water mixtures. Furthermore, if hydrogen bonding is the predominant intermolecular interaction in aqueous solutions, HB lifetimes are expected to reflect the observed association bias. Indeed, the water-water HB lifetimes τ_{ww} for all water molecules were found to increase substantially when increasing the methanol content in the mixture, whereas the methanol-methanol HB lifetimes τ_{mm} were shown to be consistently lower than the HB lifetimes of both the water-water (τ_{ww}) and the mixed methanol–water (τ_{mw}) interactions. These results suggest incomplete mixing at the molecular level as a source for the excess effects observed for methanol–water mixtures. Thereby nearest neighbor relationships $\boldsymbol{M}_{ii}$ quantify the degree of molecular segregation and the bias witnessed for the different molecule types in simple, pictorial terms, based on a single parameter, nearest neighbor relationships, which is derived from first-principles on the molecular scale.

Hydrophobicity in the context of percolation

Neither of the above mentioned models offers any explanation for the localization and the molecular causes for the minimum in excess properties of methanol–water mixtures, such as entropy or molecular self-diffusion. Pure water and aqueous solutions with high water content are known to percolate [49–51], which implies that a continuous system-wide water cluster exists, in which all water molecules are interconnected via hydrogen bonds. For every point in time a lattice of water molecules can be constructed, in which a hydrogen bond between lattice points may be defined as "occupied" or "empty" [52]. Bond percolation persists as long as a single continuous graph can be constructed that connects all lattice points within the system. A percolation threshold $\boldsymbol{p}_{c=}\ \boldsymbol{\chi}^{c}_{wat}$ close to equimolar mixture has been reported for methanol–water mixtures [53, 54], which was confirmed by our clustering analysis. The discrepancy between the number of maximal and minimal observable clusters in our largest cluster analysis ($\boldsymbol{N}_{\max}$ and $\boldsymbol{N}_{\min}$, respectively) suggests that the transition from one

continuous water cluster (percolation) to isolated water clusters is not precisely localized. For χ_{wat}=0.6, system-wide water molecule clusters (e.g., cluster size N_{max}=542) exist temporarily, while at other times only isolated largest clusters can be found in the mixtures (e.g., cluster size N_{max}= 98). It should also be noted that the presented data does not consider how methanol is involved in the hydrogen network, which might slightly lower the percolation threshold with the formation of bi-percolating networks [53].

A relation between percolation and anomalies in thermodynamic quantities has previously been suggested [53], and hydrogen bonding has been linked to macroscopic excess properties at critical mixture compositions [55]. A crossover point for different hydrogen bonding environments from water-rich to methanol-rich environment was previously proposed at χ_{wat}~0.4 [56]. Since the percolation threshold for water molecules at χ_{wat}~0.5 coincides with the minimum in molecular self-diffusion for both methanol and water, it is assumed that the mobility of molecules, and thus entropy, is directly affected by percolation. The HB lifetimes analysis underscores this hypothesis, particularly τ_{ww}, which depends linearly on χ_{wat} for χ_{wat}<0.5 and exponentially for χ_{wat}>0.5, indicating a fundamental change in hydrogen bonding dynamics at the percolation threshold. The difference in increased τ_{ww} for bulk water in comparison to clathrate-like water suggests that this effect arises due to the significant enhancement of water-water hydrogen bonding in the bulk, which is exactly the opposite effect of what would be expected of clathrate-like hydration and thus is in stark contradiction to the Frank and Evans model. It is however in agreement with the view that the loss of hydrogen bonding drives the segregation of nonpolar moieties from water [2] and offers a fresh perspective on how enthalpic and entropic contributions to the free energy of solvation may be interpreted for methanol–water mixtures.

In general, hydrophobicity in aqueous solutions is considered to be a multifaceted problem [2, 3], where the enthalpic breaking of hydrogen bonds dominates for large solutes, whereas for small solutes in aqueous solution, like methanol–water mixtures, the free energy is perceived to be mainly affected by entropic reordering of hydrogen bonds. In methanol–water mixtures, entropic reordering of water molecules to maintain bulk-like tetrahedral hydrogen bond coordination may obviously only take place above the percolation threshold (χ_{wat}>0.5), where a sufficient number of water molecules are available as bonding partners. Therefore, the formation or the breakdown of the system-wide hydrogen bonding network have a major effect on hydrogen bond dynamics. On the basis of our findings, we suggest that the percolation threshold is not only a critical threshold for excess properties such as molecular self-diffusion, but is also a divisive threshold for two distinctively different hydrophobicity regimes. A possible pictorial model is described in the following subsections.

Molecular mechanism of water diffusion

The observed minimum of molecular self-diffusion of water at χ_{wat}≈0.5 could thus be explained: For high water content (χ_{wat}>0.5) in the methanol–water mixture, the percolation in the system-wide hydrogen bonding network persists as the association bias between water molecules becomes more prevalent and individual hydrogen bonds are maintained for longer durations. Decreasing the water content in the mixture coincides with an increasing nearest neighbor bias M_{ww} and rising HB lifetimes τ_{ww}, suggesting an enhanced water-water interaction, thus reducing the overall mobility of water molecules as fewer binding partners are available. Just above the percolation threshold (χ^c_{wat}>0.5), the network resembles a tight mesh of water molecules and its restricted mobility explains the minimal diffusion coefficient and the high degree of structural order. Below the percolation threshold (χ_{wat}< 0.5) the hydrogen bonding network breaks down and we find isolated water clusters, the size of which decrease with decreasing water content. While at χ_{wat}=0.4 the majority of clusters consist of 10–50 water molecules, at χ_{wat}=0.1 the majority of clusters found are below size 10 (Online resource Fig. S7B). For clusters of decreasing diameter, the observed increase in diffusion could be explained by the Einstein-Stokes relation. This would also explain the significant increase of the HB lifetimes τ_{ww} for χ_{wat}<0.5 between water molecules in the bulk water group, while τ_{ww} in the clathrate-like water group remain at relatively low levels.

Molecular mechanism of methanol diffusion

Nearest neighbor relationships (M_{mm} and M_{mw}) suggest that methanol molecules preferably associate with water molecules in the mixture rather than with other methanol molecules. This conclusion is supported by the fact that HB lifetimes τ_{mw} between methanol and water molecules are consistently higher than HB lifetimes τ_{mm} between methanol molecules. In contrast to water, pure methanol does not form a system-wide network, but clusters into small rings or chains [57, 58]. At low water content, water molecules do not perturb this local structure, which is in agreement with the constant HB lifetime τ_{mm} between methanol molecules at χ_{met}>0.5. As the water content increases, the size of the water clusters increases and methanol molecules increasingly interact with the water clusters, which could explain an overall decrease in diffusion of methanol adapting to decreasing diffusion of water. At the percolation threshold χ^c_{wat}≈0.5, the formation of a system-wide HB network of water significantly perturbs the existing methanol structures by spatial constraints. The decreasing methanol–water HB lifetimes could be explained by competing water-water HB in the system-wide network, which would effectively result in increased mobility of methanol molecules.

Conclusions

Clathrate-like hydration as a source for excess entropy in methanol–water mixtures could not be observed. At high water content, the dynamic properties of clathrate-like water and of bulk water were similar. At low water content, the hydrogen bond lifetimes of bulk water were significantly enhanced in comparison to clathrate-like water, contradicting clathrate-like hydration. Instead, incomplete mixing was observed and quantified by nearest neighbor relationships, which offers an intuitive and pictorial way to describe hydrophobicity. Furthermore, the hydrogen bond percolation threshold ($\chi^{c}_{wat} \approx 0.5$) in the mixture was shown to coincide with the minimum in molecular self-diffusion. Two distinctively different hydrophobicity regimes were conceived: At low water content, isolated water clusters are embedded in loosely coupled methanol molecule structures, while at high water content methanol molecules are embedded in a system-wide hydrogen-bonded water network.

Acknowledgments We thank Joachim Groß (University of Stuttgart) for helpful discussions. This work was funded by SimTech Cluster of Excellence at the University of Stuttgart.

References

1. Soper AK, Dougan L, Crain J, Finney JL (2006) Excess entropy in alcohol-water solutions: a simple clustering explanation. J Phys Chem B 110(8):3472–3476
2. Chandler D (2002) Hydrophobicity: two faces of water. Nature 417(6888):491–491
3. Galli G (2007) Dissecting hydrophobicity. Proc Natl Acad Sci U S A 104(8):2557–2558
4. Jones JE (1924) On the determination of molecular fields. II. From the equation of state of a gas. Proc R Soc Lond A Math Phys Sci, Containing papers of a mathematical and physical character. 106(738):463–477
5. Frank HS, Evans MW (1945) Free volume and entropy in condensed systems.3. Entropy in binary liquid mixtures—partial molal entropy in dilute solutions—structure and thermodynamics in aqueous electrolytes. J Chem Phys 13(11):507–532
6. Kauzmann W (1959) Some factors in the interpretation of protein denaturation. Adv Protein Chem 14:1–63
7. Dixit S, Poon WCK, Crain J (2000) Hydration of methanol in aqueous solutions: a Raman spectroscopic study. J Phys Condens Matter 12(21):323–328
8. Soper AK, Finney JL (1993) Hydration of methanol in aqueous-solution. Phys Rev Lett 71(26):4346–4349
9. Wakisaka A, Komatsu S, Usui Y (2001) Solute-solvent and solvent-solvent interactions evaluated through clusters isolated from solutions: preferential solvation in water-alcohol mixtures. J Mol Liq 90(1–3):175–184
10. Jorgensen WL, Chandrasekhar J, Madura JD, Impey RW, Klein ML (1983) Comparison of simple potential functions for simulating liquid water. J Chem Phys 79(2):926–935
11. Meng EC, Kollman PA (1996) Molecular dynamics studies of the properties of water around simple organic solutes. J Phys Chem 100(27):11460–11470
12. Morrone JA, Hasllinger KE, Tuckerman ME (2006) Ab initio molecular dynamics simulation of the structure and proton transport dynamics of methanol—water solutions. J Phys Chem B 110(8):3712–3720. doi:10.1021/jp0554036
13. van Erp TS, Meijer EJ (2001) Hydration of methanol in water. A DFT-based molecular dynamics study. Chem Phys Lett 333(3–4):290–296
14. Dixit S, Crain J, Poon WCK, Finney JL, Soper AK (2002) Molecular segregation observed in a concentrated alcohol-water solution. Nature 416(6883):829–832
15. Finney JL, Bowron DT, Daniel RM, Timmins P, Roberts MA (2003) Molecular and mesoscale structures in hydrophobically driven aqueous solutions. Biophys Chem 105(2–3):391–409. doi:10.1016/s0301-4622(03)00104-2
16. Guo JH, Luo Y, Augustsson A, Kashtanov S, Rubensson JE, Shuh DK, Agren H, Nordgren J (2003) Molecular structure of alcohol-water mixtures. Phys Rev Lett 91(15)
17. Berendsen HJC, Postma JPM, Vangunsteren WF, Dinola A, Haak JR (1984) Molecular-dynamics with coupling to an external bath. J Chem Phys 81(8):3684–3690
18. Hockney RW, Goel SP, Eastwood JW (1974) Quiet high-resolution computer models of a plasma. J Comput Phys 14(2):148–158
19. Ryckaert JP, Ciccotti G, Berendsen HJC (1977) Numerical-integration of cartesian equations of motion of a system with constraints—molecular-dynamics of n-Alkanes. J Comput Phys 23(3):327–341
20. Essmann U, Perera L, Berkowitz ML, Darden T, Lee H, Pedersen LG (1995) A smooth particle mesh Ewald method. J Chem Phys 103(19):8577–8593
21. York DM, Darden TA, Pedersen LG (1993) The effect of long-range electrostatic interactions in simulations of macromolecular crystals—a comparison of the Ewald and truncated list methods. J Chem Phys 99(10):8345–8348
22. Jorgensen WL, Maxwell DS, TiradoRives J (1996) Development and testing of the OPLS All-atom force field on conformational energetics and properties of organic liquids. J Am Chem Soc 118(45):11225–11236
23. Hess B, Kutzner C, van der Spoel D, Lindahl E (2008) GROMACS 4: Algorithms for highly efficient, load-balanced, and scalable molecular simulation. J Chem Theory Comput 4(3):435–447
24. van der Spoel D, Lindahl E, Hess B, Groenhof G, Mark AE, Berendsen HJC (2005) GROMACS: Fast, flexible, and free. J Comput Chem 26(16):1701–1718
25. Dzugutov M (2001) A universal scaling law for atomic diffusion in condensed matter. Nature 411(6838):720–720
26. Allen M.P. TDJ (1987) Computer Simulations of Liquids Oxford University Press Inc, Oxford,
27. Luzar A (2000) Resolving the hydrogen bond dynamics conundrum. J Chem Phys 113(23):10663–10675
28. Rapaport DC (1983) Hydrogen-bonds in water network organization and lifetimes. Mol Phys 50(5):1151–1162
29. van der Spoel D, van Maaren PJ, Berendsen HJC (1998) A systematic study of water models for molecular simulation: derivation of water models optimized for use with a reaction field. J Chem Phys 108(24):10220–10230
30. Halle B, Wennerstrom H (1981) Interpretation of magnetic-resonance data from water nuclei in heterogeneous systems. J Chem Phys 75(4):1928–1943
31. Struis R, Debleijser J, Leyte JC (1987) Dynamic behavior and some of the molecular properties of water molecules in pure water and in MgCl2 solutions. J Phys Chem 91(6):1639–1645
32. Derlacki ZJ, Easteal AJ, Edge AVJ, Woolf LA, Roksandic Z (1985) Diffusion-coefficients of methanol and water and the mutual diffusion-coefficient in methanol water solutions at 278-K and 278-K. J Phys Chem 89(24):5318–5322

33. Mikhail SZ, Kimel WR (1961) Densities and viscosities of methanol–water mixtures. J Chem Eng Data 6(4):533–537. doi:10.1021/je60011a015
34. Wensink EJW, Hoffmann AC, van Maaren PJ, van der Spoel D (2003) Dynamic properties of water/alcohol mixtures studied by computer simulation. J Chem Phys 119(14):7308–7317. doi:10.1063/1.1607918
35. Lankau T, Konrad O (2007) Hydrophobic solvation: aqueous methane solutions. J Chem Educ 84(5):864
36. Bowron DT, Filipponi A, Roberts MA, Finney JL (1998) Hydrophobic hydration and the formation of a clathrate hydrate. Phys Rev Lett 81(19):4164–4167
37. Titantah JT, Karttunen M (2012) Long-time correlations and hydrophobe-modified hydrogen-bonding dynamics in hydrophobic hydration. J Am Chem Soc 22:9362–9368
38. Rezus YLA, Bakker HJ (2007) Observation of immobilized water molecules around hydrophobic groups. Phys Rev Lett 99(14):148301
39. Jorgensen WL, Buckner JK (1987) Use of statistical perturbation-theory for computing solvent effects on molecular-conformation—butane in water. J Phys Chem 91(24):6083–6085
40. Kincaid RH, Scheraga HA (1982) Acceleration of convergence in Monte-Carlo simulations of aqueous-solutions using the metropolis algorithm—hydrophobic hydration of methane. J Comput Chem 3(4):525–547
41. Rosenberg RO, Mikkilineni R, Berne BJ (1982) Hydrophobic effect on chain folding—the trans to gauche isomerization of normal-butane in water. J Am Chem Soc 104(26):7647–7649
42. Rossky PJ, Zichi DA (1982) Molecular librations and solvent orientational correlations in hydrophobic phenomena. Faraday Symp Chem Soc 17:69–78
43. Rossky PJ, Friedman HL (1980) Benzene-benzene interaction in aqueous-solution. J Phys Chem 84(6):587–589
44. Laage D, Stirnemann G, Hynes JT (2009) Why water reorientation slows without iceberg formation around hydrophobic solutes. J Phys Chem B 113(8):2428–2435
45. Qvist J, Halle B (2008) Thermal signature of hydrophobic hydration dynamics. J Am Chem Soc 130(31):10345–10353
46. Dzugutov M (1996) A universal scaling law for atomic diffusion in condensed matter. Nature 381(6578):137–139
47. Pratt LR (2002) Molecular theory of hydrophobic effects: "She is too mean to have her name repeated". Annu Rev Phys Chem 53:409–436
48. Hummer G, Garde S, Garcia AE, Pratt LR (2000) New perspectives on hydrophobic effects. Chem Phys 258(2–3):349–370
49. Blumberg RL, Stanley HE, Geiger A, Mausbach P (1984) Connectivity of hydrogen-bonds in liquid water. J Chem Phys 80(10):5230–5241
50. Geiger A, Stillinger FH, Rahman A (1979) Aspects of the percolation process for hydrogen-bond networks in water. J Chem Phys 70(9):4185–4193
51. Stanley HE, Teixeira J (1980) Interpretation of the unusual behavior of H2O and D2O at low-temperatures—tests of a percolation model. J Chem Phys 73(7):3404–3422
52. Shante VKS, Kirkpatrick S (1971) Introduction to percolation theory. Adv Phys 20(85):325
53. Dougan L, Bates SP, Hargreaves R, Fox JP, Crain J, Finney JL, Reat V, Soper AK (2004) Methanol–water solutions: a Bi-percolating liquid mixture. J Chem Phys 121(13):6456–6462. doi:10.1063/1.1789951
54. Bako I, Megyes T, Balint S, Grosz T, Chihaia V (2008) Water–methanol mixtures: topology of hydrogen bonded network. Phys Chem Chem Phys 10(32):5004–5011. doi:10.1039/b808326f
55. Sato T, Chiba A, Nozaki R (2000) Hydrophobic hydration and molecular association in methanol–water mixtures studied by microwave dielectric analysis. J Chem Phys 112(6):2924–2932
56. Pascal TA, Goddard WA Hydrophobic segregation, phase transitions and the anomalous thermodynamics of water/methanol mixtures. J Phys Chem B 116 (47):13905–13912
57. Haughney M, Ferrario M, McDonald IR (1987) Molecular-dynamics simulations of liquid methanol. J Phys Chem 91(19):4934–4940
58. Yamaguchi T, Hidaka K, Soper AK (1999) The structure of liquid methanol revisited: a neutron diffraction experiment at −80 °C and +25 °C. Mol Phys 97(4):603–605